

Stabilization of DNA-encapsulating Droplets through Negative Charge at the Droplet Interface

Mayu Shono,¹ Fumika Fujita,² Kenichi Yoshikawa,^{2,3} and Akihisa Shioi*¹

¹Department of Chemical Engineering and Materials Science, Doshisha University, Kyoto 610-0321, Japan

²Faculty of Life and Medical Sciences, Doshisha University, Kyoto 610-0394, Japan

³Center for Integrative Medicine and Physics, Institute for Advanced Study, Kyoto University, Kyoto 606-8501, Japan

E-mail: ashioi@mail.doshisha.ac.jp

It was found that stable cell-sized droplets entrapping DNA molecules are spontaneously generated through micro segregation. To clarify the mechanism, we performed measurements of the electrification by adapting a polymer solution with polyethylene glycol/dextran. We determined the Donnan potential for macroscopic phase segregation in both the presence and absence of DNA, together with the measurements of Zeta potentials of the microphase solution with number of small droplets. We confirmed that the droplets entrapping DNA are negatively charged.

Keywords: Cell-sized droplets |
Water/water phase separation |
Electrification of droplets

Living cells maintain their activity through highly crowded intracellular solutions with 30–40 wt/wt % of biomaterials, such as DNA, RNA, and proteins.^{1,2} Recently, water/water (w/w) microdroplets generated by aqueous two-phase systems (ATPS) and the crowding effects on the cytoplasm have garnered research attention. Numerous studies have reported on microdroplets generated through microphase separation or liquid–liquid phase separation (LLPS) as models for membrane-less organelles, including nucleoli, Cajal bodies, nuclear speckles, paraspeckles, nuclear bodies, P-bodies, and stress granules.^{3–12} The microdroplets generated by phase transition are unstable and tend to undergo macroscopic phase separation through coalescence or coarsening, according to general thermodynamical arguments. In contrast, we found that w/w microdroplets entrapping DNA and F-actin in a spontaneous manner are rather stable and maintain the cell-sized scale for more than several weeks.⁵ The main purpose of this study was to clarify the underlying physicochemical mechanism of the stability of cell-sized microdroplets entrapping DNA. We investigated the effect of DNA on the stability of microdroplets generated in a self-organized manner accompanied by phase separation in ATPS with binary hydrophilic polymers. It is well known^{13–16} that aqueous solution of polyethylene glycol (PEG) and dextran (DEX) is a typical example of ATPS, where the driving force is attributable to the depletion interaction with conformational entropy of polymers. In past studies,^{5,6,9,17} we reported that long DNA molecules above several hundred base pairs (bps) are entrapped into DEX-rich droplets in a spontaneous manner, which has been attributed to the different manner of macromolecular packing between PEG-rich and DEX-rich phases caused by depletion effect due to the large difference of polymer flexibility. Here, we study how DNA incorporated in DEX-rich droplets prevents mutual fusion in a quantitative manner. We will argue the stabilization of the microdroplets in relation to the electronic charge effect on the droplets induced by the dissolved DNA.

An ATPS consisting of a chain-structured flexible polymer (PEG, MW = 6,000; Fuji Film Wako Pure Chemical Industries, Osaka, Japan) and a branched stiff polymer (DEX, MW = 200,000; Fuji Film Wako Pure Chemical Industries) was used. The polymer composition was 5 wt %:5 wt % PEG:DEX, corresponding to a phase-separated state near the binodal line of phase separation.¹⁸ DNA molecules from Salmon sperm (500–1,000 bp; Fuji Film Wako Pure Chemical Industries) were used. Crystalline DNA powder was dissolved in nuclease-free water and added to the PEG/DEX solution. Tris-HCl (pH 7.5; Nippon Gene, Tokyo, Japan) was added to the solution at a concentration of 8 mM. A centimeter-sized plastic cuvette was used to observe the macroscopic phase separation. Glass slides (confinement size: 4 × 18 mm; depth: 90 μm) were used for fluorescence microscopy. The DEX-rich phase was labeled with fluorescein isothiocyanate–DEX (FITC–DEX; excitation wavelength [Ex]: 488 nm; emission wavelength [Em]: 520 nm; Sigma-Aldrich, St. Louis, MO, USA). Gelgreen (Ex: 500 nm, Em: 530 nm; Biotium Inc., Fremont, CA, USA) was used as a fluorescent dye for DNA. The images observed under a fluorescence microscope (Olympus BX51; Olympus Co., Tokyo, Japan) were captured using a charge-coupled device digital camera (C11440-36U; Hamamatsu Photonics, Hamamatsu, Japan). Zetasizer Ultra with a capillary cell (DTS1070) (Malvern Panalytical, Malvern, UK) was used to measure the zeta potential. For DEX-rich droplets, the refractive index was 1.33.¹⁹ For PEG-rich (continuous) phase, the refractive index, dielectric constant, and measured viscosity (at approximately 23 °C) were 1.34, 70, and 2.63 mPa s, respectively.^{20,21} The interfacial potential between the DEX-rich- and PEG-rich phases was measured using two Ag–AgCl electrodes immersed in the two phases. A water quality analyzer (LAQUA; HORIBA, Kyoto, Japan) was used as potentiometer.

Figure 1a shows the phase separation of PEG/DEX solution without DNA (control, upper panels) and with DNA (lower panels) in a centimeter-sized plastic cuvette at room temperature (23 °C). Immediately after mixing, both solutions, without and with DNA, were cloudy, indicating the formation of a very large number of micro droplets. At 15 min after the mixing, macroscopic phase separation became evident because of the formation of two phases with the upper phase still cloudy. The upper and lower phases corresponded to the PEG- and DEX-rich phases, respectively. At 120 min after the mixing, the upper (PEG-rich) phase became clear. No remarkable effect of dissolved DNA was observed in the macroscopic phase separation. Figure 1b shows the microscopy images of the growth of DEX-rich droplets under phase separation for quasi-2-dimensional space between planar glass slides. Fluorescence microscopy revealed that DNA was spontaneously localized in the DEX-rich droplets through the phase separation (right panel). DEX-rich droplets without DNA grew in size, whereas entrapping DNA prevented size growth.

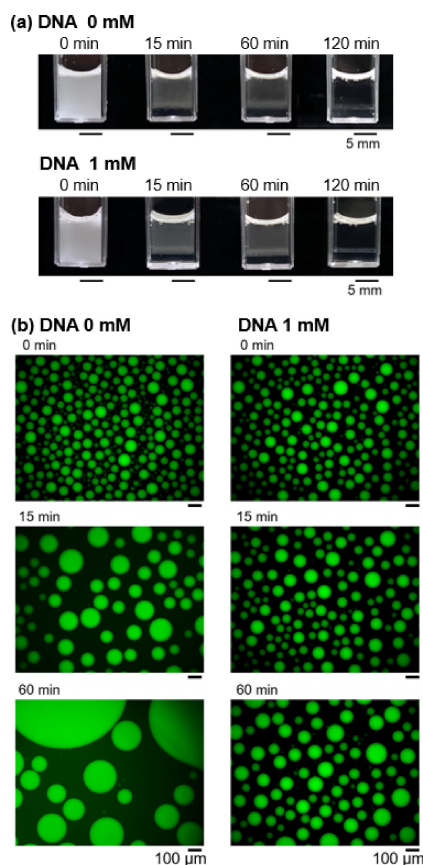


Figure 1. Phase separation of solutions (without DNA [control] and with 1 mM DNA) at room temperature (23 °C) (a) in a centimeter-sized plastic cuvette. Immediately after mixing, the solutions become cloudy for both cases. Macroscopic phase separation becomes evident at 15 min after the mixing. The upper and lower phases correspond to the PEG- and DEX-rich phases, respectively. (b) Fluorescence microscopy images of droplet growth under quasi-2-dimensional phase separation between the glass slides (depth: 90 μm). The left and right panels are the results of the control and with DNA solutions, respectively. The polymer composition is 5 wt %:5 wt % PEG:DEX. Salmon sperm DNA (500–1,000 bp) is used at 1 mM. The fluorescence is caused by DEX-rich phase (labeled with fluorescein isothiocyanate-DEX, left panel); the DNA is labeled with Gelgreen (right panel). DNA is localized into DEX-rich droplets. These DNA-encapsulating droplets inhibit the growth in the glass slides, but no remarkable difference is observed in the cuvettes.

Figure 2 displays the distribution of diameter of the droplets shown in Figure 1b, as a function of time. Just after the mixing (at 0 min), many small droplets below the size of 100 μm were generated, where their size distributions were essentially the same between the conditions without and with DNA. In contrast, the difference in the size distribution became marked over time: without DNA droplets became larger with time but with DNA increase of their size was suppressed significantly. Although droplets without DNA coalesced and became larger over time, droplet growth was inhibited by entrapping DNA.

Figure 3 shows the zeta potential of DEX-rich droplets at 23 °C, measured at 0, 15, 60 min after mixing. The probability density of the zeta potential distribution normalized by its maxi-

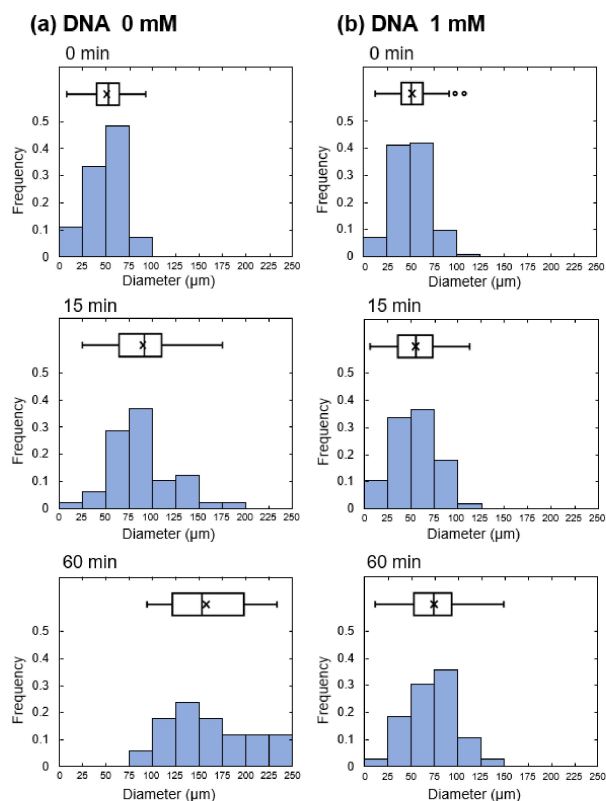


Figure 2. Histograms of droplet diameter as a function of time of the (a) control and (b) with DNA samples. These histograms were made based on the fluorescence microscopy results shown in Figure 1b. Mean value (X) and distribution (bar) of the droplet diameter are shown as box plots. DEX-rich droplets without DNA grow, while entrapping DNA prevent the growth.

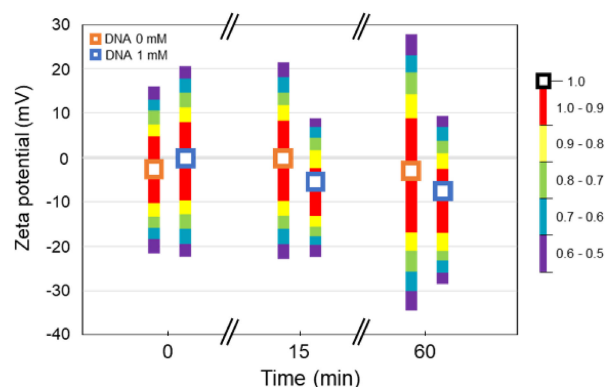


Figure 3. Effect of entrapping DNA on the zeta potential of DEX-rich droplets at different times. The probability density of distribution of the zeta potential normalized by its maximum value is represented by the color bar (contour line). The zeta potential of the control is close to zero even at 60 min after mixing. In contrast, the zeta potential of the sample with DNA becomes more negative over time.

imum value is represented by a colored bar (contour line). A typical graphical representation is shown in Figure S1. The zeta potential of the control sample (without DNA) was distributed around zero

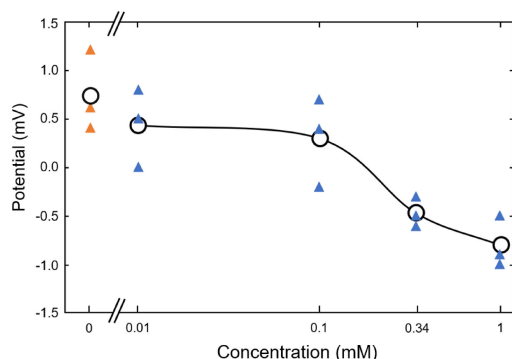


Figure 4. Correlation of electrostatic potential difference between PEG-rich and DEX-rich phases with DNA concentration under obvious macroscopic phase separation after standing overnight (for example, see Figure 1a where the macroscopic interface between the two phases is obvious even after shorter standing period with 120 min). The absolute value of negative potential increases with the DNA concentration. The experiments were performed three times. The mean values (open circles) and the measured data (closed triangles) are shown.

even after 60 min. In the presence of DNA, just after the mixing (at 0 min) the zeta potential was almost zero mV. With time (15 and 60 min), the zeta potential became more negative over time. Such time-dependent changes of the zeta potential with and without DNA correspond well to the time dependent increase of the droplet sizes as in Figure 2(b) and Figure 3, suggesting that the surface of DEX-rich droplets tends to be negatively charged by entrapping DNA accompanied with the stabilization through the suppression effect against fusion among the droplets. Here, it is also to be noted that the distribution of the zeta potential becomes narrower at 15 and 60 min, which is attributable to such stabilization effect on the negatively charged droplets.

Figure 4 shows the electrostatic potential difference between the PEG-rich and DEX-rich phases as a function of DNA concentration under macroscopic phase separation after standing overnight. The upper and lower phases were clear already at 120 min as shown in Figure 1a. The negative potential difference indicates that the potential of the DEX-rich phase is lower than that of the PEG-rich phase. This negative potential difference increases with the DNA concentration.

In summary, the following has become clear: 1) Micro- or cell-sized droplets of DEX-rich solution are stabilized by incorporating DNA molecules (Figures 1 and 2).^{5,6} 2) A negative zeta potential on the order of -10 mV is generated for the DNA entrapped DEX-rich droplets (Figure 3). 3) The interfacial electric potential (Donnan potential) of the macroscopic interface was negative, on the order of -1 mV, for the DEX-rich phase with respect to the PEG-rich phase (Figure 4).

The results of this study suggest that the stabilization of phase-segregated droplets entrapping DNA is attributable to the generation of a negative electric potential on the surface of the droplets.^{22,23} We now discuss the mechanism of a negative electric potential occurrence in the droplets. For both micro- and macro phase segregation (as shown in Figures 3 and 4, respectively), ionic species can migrate through the interface between the DEX-rich- and PEG-rich solutions, except for the negatively charged DNA molecules that prefer the DEX-rich phase. Such

selectivity of double-stranded DNA is attributable to different assembly manner of PEG and DEX under crowded conditions. For a crowded DEX-rich solution, nanosized void spaces exist because of DEX's stiff backbone and branched conformation. Thus, double-stranded DNA with a diameter of approximately 2 nm and persistence length of approximately 50 nm can persist with a rather small entropic penalty owing to the depletion effect.^{24,25} In contrast, the PEG-rich solution is fully occupied by flexible coil chains, and the DNA chains tend to be excluded. Based on these considerations, the observed electric potential difference between the two aqueous phases can be interpreted in terms of Donnan potential.^{26–30} Notably, the membrane potential in biosystems is usually described by the diffusion potential with barrier effects due to small ions. In an LLPS system, the Donnan potential is used, instead of the diffusion potential, because there is no insulator thin film at the interface. The Donnan potential is given by eq 1 under the approximation that the ion concentrations C_s are almost the same in the two aqueous phases:^{26–30}

$$\Psi \approx \frac{RT}{F} \frac{z\Delta C_p}{2C_s} \quad (1)$$

where R , T , F , and z are universal gas constant, absolute temperature, Faraday constant, and valence, respectively ($RT/F \approx 26$ mV at 23 °C). $z\Delta C_p$ is the difference in the electronic charge of polyelectrolytes between the two phases, presented in units of molarity, and is estimated to be approximately 70% of the concentration of the phosphate group of double-stranded DNA in the DEX-rich phase by considering the effect of counter ion condensation.^{31,32} Thus, we assumed that $z\Delta C_p$ is approximately 1 mM considering the enrichment of DNA in the DEX-rich phase. Under our experimental conditions, the ion concentration C_s was approximately 10 mM (the buffer was 8 mM Tris-HCl, and there were additional ions from the DNA sample). We thus calculated Ψ to be approximately -1.3 mV for the electric potential of the DEX-rich phase with DNA relative to the PEG phase. This value agrees well with the experimental electric potential for the macroscopic phase separation of approximately 1 mV with 1 mM DNA, as shown in Figure 4. The zeta potential of the droplet emulsion was approximately 10 mV under relatively stable conditions (60 min after mixing) using 1 mM DNA (Figure 3). The theoretical Donnan potential equation (eq 1) is derived from the difference in free energy between the two phases, implying that the effect of the boundary region of the phase segregation is neglected. It should also be noted that the zeta potential does not correspond directly to the electric potential difference between the two phases, both from theoretical and experimental points of view.^{23,33,34} In addition, here zeta potential measurements were performed for a solution of droplets with a larger size dispersion, implying that the solution of a number of droplets with size dispersion exhibits non-equilibrium different from the macroscale phase separation. Further studies are required to elucidate the stabilization effect of w/w-phase-segregated droplets entrapping DNA from both experimental and theoretical points of view, which would contribute to the understanding of the intrinsic properties of living cells entrapping large amounts of polyelectrolytes, including DNA and RNA.

The results shown in Figures 1 and 2 demonstrated that the presence of DNA exhibits a marked effect inhibiting droplet growth. The zeta and interfacial potentials demonstrated that DNA caused a negative charge of a few millivolts on the surface

charge of the DEX-rich phase. Considering these results, the stabilization of droplets by DNA may be explained as follows: DNA is negatively charged by the phosphate group and when it is localized in a droplet, the phosphate group entrapped inside the droplet is ionized. Some positively charged counterions then leak out into the PEG-rich phase, by increasing the translational entropic contribution. This charge separation causes a charge bias between the interior and exterior of the droplets. Consequently, the entire droplet is negatively charged, and the electrostatic repulsion prevents droplet coalescence. Therefore, negatively charged biopolymers such as DNA, RNA, and various proteins, which are present in high concentrations in living cells, may contribute to cellular structural stability and its functions. In the future, it may be of scientific significance to carry out experiments for longer periods of time over a broader range of DNA concentration and the type of polymers closer to living cells. Especially, it may be important to try to measure the interfacial electrical potential for individual droplets with different size and also with different degree of DNA entrapment by adapting micro-electrodes.

This work was supported by the Japan Society for the Promotion of Science (JSPS) KAKENHI Grants (23KJ2081, M.S.), (JP20H01877, K.Y.), and (22K03560, A.S.). We would like to thank Dr. H. Sakuta and Professor T. Kenmotsu.

Supporting Information is available on <https://doi.org/10.1246/cl.230294>.

References

- 1 S. B. Zimmerman, S. O. Trach, *J. Mol. Biol.* **1991**, *222*, 599.
- 2 R. J. Ellis, *Curr. Opin. Struct. Biol.* **2001**, *11*, 114.
- 3 H. Sakuta, N. Nakatani, T. Torisawa, Y. Sumino, K. Tsumoto, K. Oiwa, K. Yoshikawa, *Commun. Chem.* **2023**, *6*, 80.
- 4 H. Sakuta, F. Fujita, T. Hamada, M. Hayashi, K. Takiguchi, K. Tsumoto, K. Yoshikawa, *ChemBioChem* **2020**, *21*, 3323.
- 5 N. Nakatani, H. Sakuta, M. Hayashi, S. Tanaka, K. Takiguchi, K. Tsumoto, K. Yoshikawa, *ChemBioChem* **2018**, *19*, 1370.
- 6 M. Shono, G. Honda, M. Yanagisawa, K. Yoshikawa, A. Shioi, *Small* **2023**, *19*, 2302193.
- 7 M. Shono, R. Ito, F. Fujita, H. Sakuta, K. Yoshikawa, *Sci. Rep.* **2021**, *11*, 23570.
- 8 A. T. Rowland, C. D. Keating, *Soft Matter* **2021**, *17*, 3688.
- 9 K. Tsumoto, H. Sakuta, K. Takiguchi, K. Yoshikawa, *Biophys. Rev.* **2020**, *12*, 425.
- 10 S. Shil, M. Tsuruta, K. Kawauchi, D. Miyoshi, *BioTech* **2023**, *12*, 26.
- 11 Y. Sato, T. Sakamoto, M. Takinoue, *Sci. Adv.* **2020**, *6*, eaba3471.
- 12 A. Zinchenko, E. Inagaki, S. Murata, *ACS Omega* **2019**, *4*, 458.
- 13 P. Å. Albertsson, *Anal. Biochem.* **1987**, *161*, 227.
- 14 J. F. B. Pereira, J. A. P. Coutinho, *Elsevier* **2020**, 157.
- 15 F. Dumas, J.-P. Benoit, P. Saulnier, E. Roger, *J. Colloid Interface Sci.* **2021**, *599*, 642.
- 16 C. D. Crowe, C. D. Keating, *Interface Focus* **2018**, *8*, 20180032.
- 17 T. Nishio, Y. Yoshikawa, K. Yoshikawa, *PLoS One* **2021**, *16*, e0261736.
- 18 K. Tsumoto, M. Arai, N. Nakatani, S. N. Watanabe, K. Yoshikawa, *Life* **2015**, *5*, 459.
- 19 C. F. Snyder, H. S. Isbell, M. Dryden, N. B. Holt, *J. Res. Natl. Bur. Stand.* **1954**, *53*, 131.
- 20 B. de Sá Costa, E. E. Garcia-Rojas, J. S. dos Reis Coimbra, J. A. Teixeira, J. Telis-Romero, *J. Chem. Eng. Data* **2014**, *59*, 339.
- 21 B. Y. Zaslavsky, L. M. Miheeva, M. N. Rodnikova, G. V. Spivak, V. S. Harkin, A. U. Mahmudov, *J. Chem. Soc., Faraday Trans. 1* **1989**, *85*, 2857.
- 22 B. T. Nguyen, T. Nicolai, L. Benyahia, *Langmuir* **2013**, *29*, 10658.
- 23 T. J. Welsh, G. Krainer, J. R. Espinosa, J. A. Joseph, A. Sridhar, M. Jahnel, W. E. Arter, K. L. Saar, S. Alberti, R. Collepardo-Guevara, T. P. J. Knowles, *Nano Lett.* **2022**, *22*, 612.
- 24 S. Asakura, F. Oosawa, *J. Polym. Sci.* **1958**, *33*, 183.
- 25 M. Negishi, M. Ichikawa, M. Nakajima, M. Kojima, T. Fukuda, K. Yoshikawa, *Phys. Rev. E* **2011**, *83*, 061921.
- 26 M. Vis, B. H. Ern e, R. H. Tromp, *Biointerphases* **2016**, *11*, 018904.
- 27 M. Vis, V. F. D. Peters, E. M. Blokhuis, H. N. W. Lekkerkerker, B. H. Ern e, R. H. Tromp, *Phys. Rev. Lett.* **2015**, *115*, 078303.
- 28 J. Landman, M. P. M. Schelling, R. Tuinier, M. Vis, *J. Chem. Phys.* **2021**, *154*, 164904.
- 29 M. Vis, V. F. D. Peters, B. H. Ern e, R. H. Tromp, *Macromolecules* **2015**, *48*, 2819.
- 30 M. Vis, V. F. D. Peters, R. H. Tromp, B. H. Ern e, *Langmuir* **2014**, *30*, 5755.
- 31 F. Oosawa, *Biopolymers* **1968**, *6*, 1633.
- 32 G. S. Manning, *J. Chem. Phys.* **1969**, *51*, 924.
- 33 F. Paratore, V. Bacheva, G. V. Kaigala, M. Bercovici, *Proc. Natl. Acad. Sci. U.S.A.* **2019**, *116*, 10258.
- 34 R. J. Hunter, *Zeta Potential in Colloid Science: Principles and Applications*, Third printing, Academic Press, San Diego, **1988**.